Navigational strategies underlying temporal phototaxis in *Drosophila* larvae

Running title: Temporal phototaxis in *Drosophila* larvae

Maxwell L. Zhu[1,2], Kristian J. Herrera[2,3], Katrin Vogt[1,3] and Armin Bahl[2,3,*]

[1] Department of Physics, Harvard University, 17 Oxford Street, Cambridge, MA 02138, USA

[2] Department of Molecular and Cellular Biology, Harvard University, 16 Divinity Avenue, Cambridge, MA 02138, USA

[3] Center for Brain Science, Harvard University, 52 Oxford Street, Cambridge, MA 02138, USA

*Correspondence: arminbahl@fas.harvard.edu

Keywords: larval *Drosophila*, behavior, navigation, phototaxis, modeling

Summary statement

Using a novel closed-loop behavioral assay, we show that larval *Drosophila* can navigate light gradients using exclusively temporal cues. Analyzing and modeling their behavior in detail, we propose that larvae might achieve this by measuring luminance change over many seconds.

Abstract

Navigating across light gradients is essential for survival for many animals. However, we still have a poor understanding of the algorithms that underlie such behaviors. Here we develop a novel phototaxis assay for *Drosophila melanogaster* larvae in which light intensity is always spatially uniform but constantly updates depending on the location of the animal in the arena. Even though larvae can only rely on temporal cues in this setup, we find that they are capable of finding preferred areas of low light intensity. Analyzing movement parameters such as run and turn events, we further find that the amplitude and the frequency of turn events correlate with luminance change since the last turn, suggesting that larvae can keep a visual working memory over many seconds. An algorithmic model based on these observations could faithfully reproduce the observed behavior, suggesting that temporal integration during runs is an important element of *Drosophila* larvae phototaxis.

Introduction

Finding the preferred location or a particular sensory cue in complex natural environments is a computational challenge for many animals. Such taxis behaviors include chemotaxis, where animals seek or avoid chemical stimuli; thermotaxis, where animals aim to find cooler or warmer regions; and phototaxis, where animals approach or avoid light (Gepner et al., 2015; Gomez-Marin and Louis, 2014; Gomez-Marin et al., 2011; Kane et al., 2013; Luo et al., 2010).

Drosophila larvae are negatively phototactic throughout most of their development, preferring darker regions to brighter regions (Sawin et al., 1994). When presented with a spatially differentiated light landscape, larvae alternate between runs and turn events – during runs, larvae move relatively straight, while during turn events they sweep their heads from side to side to choose a new moving direction (Lahiri et al., 2011). Here, larvae might use light-sensitive receptors on their head to actively sample local asymmetries across space and time (Humberg and Sprecher, 2018; Humberg et al., 2018; Kane et al., 2013) to make motor decisions (Gomez-Marin and Louis, 2012; Kane et al., 2013). However, it is still unclear whether such local spatial information is necessary for *Drosophila* larvae to perform phototaxis behaviors. For example, it has been shown that zebrafish larvae can perform phototaxis in a virtual luminance landscape in which light intensity is uniform across space but changes over time according to the position of the animal (Chen and Engert, 2014). In such a purely temporal phototaxis assay, any spatial information about luminance is absent. Therefore, animals likely use some form of temporal integration and working memory to navigate these environments.

Whether *Drosophila* larvae can navigate such spatially uniform environments has not been explored. Moreover, the timescale of the computations underlying phototaxis and their role during gradient navigation remain unclear. Research on the temporal component of phototaxis has largely focused on how larvae compare sequential samples of the stimulus during single turn events by casting their heads for about 1 s (Humberg et al., 2018; Kane et al., 2013). However, there is evidence that larvae might utilize and compare information on even longer time scales. For example, during chemotaxis, larvae experiencing a decrease in the concentration of a favorable odorant over timescales longer than 5 s are more likely to initiate a turn (Gomez-Marin et al., 2011). Additionally, during chemotaxis larvae can bias run direction, even in the absence of local spatial cues (Gomez-Marin and Louis, 2014).

Here we set out to test if *Drosophila* larvae can perform temporal phototaxis. Using a virtual landscape in which luminance is always spatially uniform but depends on the location of the animal, we find that larvae can navigate towards their preferred location, the darker region.

Further dissections of the behavior reveal that they likely do so by integrating luminance change over several seconds during runs and that such cues increase the likelihood of initiating a turn event.

Materials and methods

Experimental setup

All experiments were performed using wild-type second-instar *Drosophila melanogaster* larvae collected 3–4 days after egg-laying. Larvae were raised on agarose plates with grape juice and yeast paste, with a 12h/12h light-dark cycle at 22°C and 60% humidity. Before experiments, larvae were washed in several droplets of deionized water.

Larvae were placed in the center of a circular acrylic dish (6 cm radius) which was filled with a thin layer of freshly made 2% agarose. For closed-loop tracking and presentation of visual stimuli, we used that same system that was originally developed for the study of larval zebrafish behavior (Bahl and Engert, 2019). In brief, spatially uniform whole-field illumination was presented via a projector (60 Hz, AAXA P300 Pico Projector, light intensity from 0 to 120 Lux) from below. Additionally, the scene was illuminated using infrared LED panels (940 nm panel, Cop Security). A high-speed camera (90 Hz, Grasshopper3-NIR, FLIR Systems) with an infrared filter (R72, Hoya) was used to track the larva's centroid position in real-time (**Fig. 1A**).

Two virtual light intensity landscapes were used: a "Valley" stimulus (for experimental trials) and a "Constant" stimulus (for control trials). For the "Valley" stimulus, the spatially uniform light intensity (λ) was updated according to $\lambda = (r-3)^2/9$, where r is the larva's radial distance to the center of the arena (**Fig. 1B**). We chose this profile because high luminance levels near the wall decreased the edge preference of larvae. For the "Constant" stimulus, we chose $\lambda = 0.5$, regardless of the larva's position. Both experimental and control trials lasted for 60 min. We also included a 15 min acclimation period before the trials, during which larvae were presented with constant light intensity at an intermediate level ($\lambda = 0.5$), allowing them to distribute in the arena.

Data analysis and statistics

All data analysis was performed using custom-written Python and MATLAB code. Although the temporal phototaxis effect was observed during the entire 60 min period, we found that the effect decreased over the course of the experiment (**Fig. S1A**). Therefore, we only analyzed the first 20 min of behavior data. To avoid tracking problems for the detailed analysis of speed as well as turn events, we excluded all data where larvae was within 0.3 cm of the edge (approximately one body length).

To analyze turn events (**Fig. 2A**), we calculated heading angle change by taking the angle between the direction vectors before and after a turn event. For all location-dependent analyses, the circular arena was binned in three concentric regions depending on the radius r: the "Bright center" ($r = 0 - 2\ cm$), the "Dark ring" ($r = 2 - 4\ cm$), and the "Bright edge" ($r = 4 - 6\ cm$). According to the respective brightness profile (**Fig. 1B**), the "Bright center" and the "Bright edge" were defined as the "Bright" regions, whereas the "Dark ring" was defined as the "Dark" region (**Fig. 2D,F**). Notably, we also applied the same "Dark"/"Bright" binning and nomenclature to larvae which were presented with the "Constant" stimulus, even though the arena always remained gray for those animals.

For pairwise comparisons between the experimental and control data, we used two-sample t-tests. For pairwise comparisons within groups, we used paired-sample t-tests. Prior to testing visual inspection of our data indicated that the underlying distributions were approximately Gaussian, but we did not formally test for this feature. We only discarded larvae if they did not move during the experiment or if they spent most of the time near the edge. All data analysis was done automatically in the same way for each experimental group.

Modeling

Simulations were custom-written in MATLAB. We constructed a simple algorithmic model where larvae behave like randomly moving particles with occasional turn events. Model larvae started at a random position in the arena and with a random direction vector, moving at a speed of 0.41 cm/s, the average running speed of larvae as found in our experiments (**Fig. 1F**). Simulations were performed using a loop with a timestep of $dt = 0.1\ s$. At each time step, larvae stochastically chose two possible actions. With a probability of $p = 0.01$, they performed a turn event and changed their direction vector by ±50°, the measured average heading angle (**Fig. 2B,C**). This probability was chosen to approximate the experimentally found inter-turn event interval (~10–15 s; **Fig. S1B**). Otherwise, larvae changed their heading by only ±5°, mimicking the properties of a randomly diffusing particle during runs. Edge preference was included in the model as well. If larvae reached the edge, they remained there for 10 seconds, and then chose a new random direction vector.

In close correspondence with our measured behavioral data, our model included three additional navigational rules: In "Rule 1", the amplitude of a heading angle change ω depends on the current luminance (**Fig. 2B**). If a turn event occured in the "Dark", the heading angle change amplitude (baseline = ±50°) was reduced by 5°. If it occurred in a "Bright" region, it was increased

by 5°. In “Rule 2”, the amplitude of the heading angle change ω depends on the change in light intensity since the previous turn event (**Fig. 2C**). If luminance had decreased since the last turn event (Δλ < 0), turn amplitude was reduced by 5°. Otherwise (Δλ > 0), turn amplitudes were increased by 5°. In “Rule 3”, the probability of initiating a turn event depends on the luminance change since the previous turn (**Fig. 2E**). If brightness had decreased (Δλ < 0), the probability was lowered to $p = 0.005$. If brightness had increased since the last turn (Δλ > 0), the probability was increased to $p = 0.1$. These changes in turn amplitude and turn event probability were allowed to be additive for combinations of the three rules. All eight combinations of these rules were tested (**Fig. 3C–G**), and the performance of each model was ranked using a phototaxis index (**Fig. 3H**). The phototaxis index is defined as $PI = (f_{exp} - f_{control}) / 0.5 \cdot (f_{exp} + f_{control}) \cdot 100$, where f_{exp} and $f_{control}$ are the fractions of time the experimental and control groups spent in the “Dark ring”. For all of the navigational models, n = 25 simulated larvae navigated the “Valley” stimulus and the “Constant” stimulus. For the phototaxis index calculation – which depends on the difference between two independent groups – means and variances were determined by randomly sampling difference values 1000 times (bootstrapping).

Results and discussion

Fly larvae can navigate a virtual luminance gradient

We first wanted to know whether fly larvae can perform purely temporal phototaxis, i.e. whether they can navigate a virtual light landscape in the absence of any spatial information. We placed individual larvae in a transparent dish filled with agarose and tracked their position in real-time (**Fig. 1A**). We used a projector to present spatially uniform luminance from below and coupled whole-field light levels to the larva's position in the arena in a closed-loop configuration. The whole-field brightness level followed a quadratic dependency of the larva's radial distance to the center. This stimulus resembles a virtual "Valley" in which a "Dark" ring lies in between two "Bright" regions (**Fig. 1B**). To control for naive location preference and the radial dependence of area in the circular arena, we also tested a "Constant" stimulus in which luminance levels remained gray irrespective of the position of the larva. After an initial period of presentation of constant gray, we allowed larvae to navigate either the "Valley" or the "Constant" stimulus for 60 minutes and analyzed their distribution across three concentric regions: the "Bright" center; the "Dark" ring; and the "Bright" edge.

At the beginning of each trial, larvae from both groups were mostly found near the "Bright" edge region (**Fig. 1C** and **Fig. S1A**), which is consistent with their innate edge preference. However, at the end of the trial, larvae that had navigated the "Valley" stimulus mostly ended up in the "Dark" ring region while larvae that had navigated the "Constant" stimulus largely remained in the "Bright" edge region (**Fig. 1C**). These differences between the two groups were also reflected in the raw trajectories of larvae during the time course of the experiment (**Fig. 1D**). Further analysis revealed that the fraction of time spent in the "Dark" ring region was indeed significantly different for the two groups (**Fig. 1E**). Notably, while navigating this virtual "Valley" stimulus, larvae have no spatial luminance cues, posing the question of which behavioral algorithms larvae employ. One possible explanation is that larvae simply modulate their crawling speed as a function of luminance – if larvae slow down when the environment is dark, the fraction of time spent in darker areas would be higher. To test this idea, we analyzed crawling speed for the different regions, which revealed that this feature is independent of luminance (**Fig. 1F**), suggesting that larvae might employ more complex navigational strategies.

In summary, we conclude that *Drosophila* larvae are capable of performing temporal phototaxis in the absence of any spatial information and that this behavior cannot be explained by a simple luminance-dependent modulation of crawling speed.

Larval temporal phototaxis depends on light level history

In spatially differentiated light landscapes, fly larvae are known to make movement decisions by casting their head back and forth during turn events to sample luminance differences ((Humberg and Sprecher, 2018; Humberg et al., 2018; Kane et al., 2013; Lahiri et al., 2011). However, this strategy cannot explain the results in our temporal phototaxis assay because during turn events the whole-field luminance remains constant. An alternative strategy that larvae might employ is to modulate the magnitude and/or the frequency of turn events as a function of luminance. To explore this possibility, we first sought to quantify turn events in more detail (**Fig. 2A**).

In a first set of analyses, we found that during turn events the heading angle changes were slightly larger when larvae were exposed to bright whole-field luminance compared to when they were in darkness (**Fig. 2B**). Additionally, we grouped turn events according to whether larvae experienced an overall decrease or increase in whole-field luminance since the previous turn event. Similarly, we found that heading angle changes were larger when larvae had experienced an increase in brightness since the previous turn event compared to when they had experienced a decrease (**Fig. 2C**). In general, the lengths of run periods between turn events were highly variable, ranging from ~3 s up to ~40 s (**Fig. S1B**). Therefore, we analyzed turn events grouped according to whether larvae had experienced a decrease or increase in whole-field luminance relative to 20 s before a turn event (**Fig. S1C**), corroborating our results.

Next, we sought to investigate the possibility that luminance changes might also modulate the probability of initiating a turn event, as larvae are known to initiate turn events in response to sudden brightness changes (Kane et al., 2013). We first measured the time in between consecutive turn events during periods of whole-field darkness or brightness, revealing no relationship (**Fig. 2D**). Also, we grouped turn events according to whether larvae experienced an overall decrease or increase in whole-field luminance since the previous turn event. We found that inter-turn event intervals were significantly longer when larvae had experienced a brightness decrease since the previous turn event compared to when they had experienced a brightness increase (**Fig. 2E**). We then confirmed that the magnitudes of change in light intensity during a run were non-negligible (**Fig. 2F**). These observations led us to hypothesize that larvae might accumulate information about the change in luminance over many seconds. In order to measure the time course of this behavior, we also quantified turn event probabilities as a function of luminance change relative to 5 s before a turn event. We found no relationship (**Fig. S1D**), which

makes it possible that the accumulated luminance change during this shorter time period is too small to have measurable effects.

In summary, through a detailed analysis of individual turn events, we find that larvae slightly modulate their turn angle as a function of both current luminance and change in luminance. Additionally, larvae seem to modulate the probability of initiating a turn event based on the change in luminance over many seconds.

A simple algorithmic model can explain larval temporal phototaxis

Having analyzed turn events in detail, we next wanted to know if the identified behavioral features are sufficient to explain larval temporal phototaxis. To this end, we propose three navigational rules larvae might use to navigate (**Fig. 3A**): In “Rule 1”, the heading angle change after a turn event is lower if the turn event occurs when it is dark and higher when it is bright (based on **Fig. 2B**). In “Rule 2”, the heading angle change is lower if the larva had experienced a luminance decrease since the last turn event and higher if luminance had increased during that interval (based on **Fig. 2C**). In “Rule 3”, the probability to initiate a turn event is lower when the current luminance is smaller than the luminance during the previous turn event, and higher when the luminance has increased since the previous turn event (based on **Fig. 2E**).

In order to test these navigational rules, we designed a simple algorithmic model in which larvae behaved like randomly moving particles with occasional changes in heading direction. We allowed model larvae to navigate the same virtual luminance landscapes that we used in the experiments – the “Valley” stimulus and the “Constant” stimulus – and analyzed the resulting trajectories. Consistent with our hypothesis, when all three rules were active, model larvae tended to move towards darker regions, whereas they did not do this in the absence of these rules or under control conditions (**Fig. 3B**), as we found in the experiments (**Fig. 1C**). To quantify these effects for different combinations of the proposed navigational rules, we measured the time spent within each region as we did for our experimental data (**Fig. 1E**). As expected, without these rules, the distribution of larvae in the “Valley” stimulus was the same as for the “Constant” stimulus (**Fig. 3C**). Interestingly, adding “Rule 1” or “Rule 2” to our model was insufficient to produce the observed behavior (**Fig. 3D,E**), suggesting that modulating the heading angle change alone cannot explain temporal phototaxis. We next tested “Rule 3” and found that model larvae were now able to find the “Dark” ring region (**Fig. 3F**), as was the case when we combined all three navigational rules (**Fig. 3G**), suggesting that altering the probability of initiating a turn event is necessary for temporal phototaxis. Finally, in order to compare the performances of all eight

combinations of the navigational rules, we calculated a phototaxis index, defined to be the difference of time spent in the “Dark” ring between experimental and control groups (**Fig. 3H**). We found that all models without “Rule 3” failed to reproduce the behavior, but any model using “Rule 3” worked well. Specifically, adding “Rule 2” to “Rule 3” improved the phototaxis index, and simultaneously adding “Rule 1” improved it even further, approaching the experimentally observed value.

Finally, even though we did not find this feature in our experiments (**Fig. 2D**), we tested if larval temporal phototaxis might be explained by modulating the probability of initiating a turn event as a function of current luminance. We incorporated this idea as “Rule 4” in our model and found that this navigational strategy could not explain the behavior (**Fig. S1E**).

In summary, after implementing the experimentally observed navigational rules in a simple computational model, we propose that a critical element of larval temporal phototaxis is their ability to adjust their turn event probability as a function of change in luminance.

Discussion

This study examines temporal phototaxis in *Drosophila* larvae in a closed loop assay navigating a continuous, spatially uniform light landscape. We show that even in the absence of local spatial information, larvae spend more time in regions with low light intensity, indicating that they are capable of navigating a temporal light landscape. They do so by using the change in light intensity since the previous turn event to modulate both the probability of initiating a turn and the heading angle following that turn event (**Fig. 2C, 2E**). Previous research has demonstrated that *Drosophila* larvae use temporal comparisons of light intensity during headcasts to navigate. Our results indicate that larvae are able to integrate information over longer timescales between turn events.

Our simulated model demonstrates the feasibility of using only few navigation rules to produce behavior. With just two inputs - current light intensity and change in light intensity since the previous turn event - the simulated larva's decision-making algorithm was able to convert these two inputs into a simulated behavioral output that accounted for most of the observed phototaxis behavior in the experimental data. However, only 66 percent of the phototaxis effect was explained by our model. While we chose the simplest angles and turning probabilities possible to demonstrate proof of principle, ideally these angles and turning probabilities could be distributions drawn from the experimental data. Additionally, a more detailed model could treat turn events as non-instantaneous, as well as also implement the larvae's edge preference.

Rule 2 and Rule 3 had the biggest effect on phototaxis and both require working memory on the order of 20s (**Fig. 3H**). The Simple Turn Amount rule, which involves no temporal integration, only added a small effect when combined with the others. Therefore, temporal integration of light level information is crucial for larvae navigating a spatially uniform landscape and may therefore also play an important role in modulating larval phototactic behavior in normal environment. Normal phototaxis is based on distinct spatial and temporal cues. Previous research mostly focused on how a combination of both cues can lead to phototaxis. Our results however indicate that the temporal cues, specifically the temporal integration of light intensity information on timescales of 20s, can be sufficient for the larvae to perform phototaxis. Whether this effect is as strong as phototaxis in larvae navigating a traditional, spatially differentiated landscape is an area for further research.

The wide array of genetic and molecular tools available for manipulating *Drosophila* larvae - such as single-neuron optogenetics (Hernandez-Nunez et al., 2015) - combined with connectomics (Eichler et al., 2017; Larderet et al., 2017) invite further study of the neural circuits and mechanisms responsible for long-term temporal integration in fly larvae. Previous research

has identified specific photoreceptor pathways involved in the processing of either spatial or temporal information during headcasts (Humberg et al. 2018, Humbreg and Sprecher 2018). There has also been work supporting the pivotal role of gaseous molecular messengers in regulating working memory in adult flies (Kuntz et al., 2017; Zars, 2017). The fact that an organism as simple as the fly larva seems to use working memory to perform phototaxis indicates that larvae are capable of retaining and comparing information on timescales longer than previously expected.

Acknowledgements

We are grateful to F. Engert and A. Samuel and their lab members for discussions and general support.

Author contributions

All authors contributed equally in the design of the project. A.B. built the behavioral setup. M.Z. performed experiments and analyzed data. M.Z. and A.B. wrote the manuscript with contributions from the other authors. K.J.H., K.V., and A.B. supervised the work.

Competing interests

The authors declare no competing interests.

Funding

K.V. received funding from a German Science Foundation Research Fellowship. A.B. was supported by the Human Frontier Science Program Long-Term Fellowship LT000626/2016.

Data availability

The data that support the findings of this study are available from the corresponding author upon request. Source code for data analysis and algorithmic modeling will be made available on github.

References

Bahl, A. and Engert, F. (2019). Neural circuits for evidence accumulation and decision making in larval zebrafish. *Nature Neuroscience* **in press**,.

Chen, X. and Engert, F. (2014). Navigational strategies underlying phototaxis in larval zebrafish. *Front. Syst. Neurosci.* **8**, 39.

Eichler, K., Li, F., Litwin-Kumar, A., Park, Y., Andrade, I., Schneider-Mizell, C. M., Saumweber, T., Huser, A., Eschbach, C., Gerber, B., et al. (2017). The complete connectome of a learning and memory centre in an insect brain. *Nature* **548**, 175–182.

Gepner, R., Mihovilovic Skanata, M., Bernat, N. M., Kaplow, M. and Gershow, M. (2015). Computations underlying Drosophila photo-taxis, odor-taxis, and multi-sensory integration. *Elife* **4**,.

Gomez-Marin, A. and Louis, M. (2012). Active sensation during orientation behavior in the Drosophila larva: more sense than luck. *Curr. Opin. Neurobiol.* **22**, 208–215.

Gomez-Marin, A. and Louis, M. (2014). Multilevel control of run orientation in Drosophila larval chemotaxis. *Frontiers in Behavioral Neuroscience* **8**,.

Gomez-Marin, A., Stephens, G. J. and Louis, M. (2011). Active sampling and decision making in Drosophila chemotaxis. *Nature Communications; London* **2**, 441.

Hernandez-Nunez, L., Belina, J., Klein, M., Si, G., Claus, L., Carlson, J. R. and Samuel, A. D. T. (2015). Reverse-correlation analysis of navigation dynamics in Drosophila larva using optogenetics. *Elife* **4**,.

Humberg, T.-H. and Sprecher, S. G. (2018). Two pairs of Drosophila central brain neurons mediate larval navigational strategies based on temporal light information processing. *Front. Behav. Neurosci.* **12**,.

Humberg, T.-H., Bruegger, P., Afonso, B., Zlatic, M., Truman, J. W., Gershow, M., Samuel, A. and Sprecher, S. G. (2018). Dedicated photoreceptor pathways in Drosophila larvae mediate navigation by processing either spatial or temporal cues. *Nat. Commun.* **9**, 1260.

Kane, E. A., Gershow, M., Afonso, B., Larderet, I., Klein, M., Carter, A. R., de Bivort, B. L., Sprecher, S. G. and Samuel, A. D. T. (2013). Sensorimotor structure of Drosophila larva phototaxis. *Proceedings of the National Academy of Sciences* **110**, E3868–E3877.

Kuntz, S., Poeck, B. and Strauss, R. (2017). Visual working memory requires permissive and instructive NO/cGMP signaling at presynapses in the Drosophila central brain. *Curr. Biol.* **27**, 613–623.

Lahiri, S., Shen, K., Klein, M., Tang, A., Kane, E., Gershow, M., Garrity, P. and Samuel, A. D. T. (2011). Two alternating motor programs drive navigation in Drosophila larva. *PLoS One* **6**, e23180.

Larderet, I., Fritsch, P. M. J., Gendre, N., Neagu-Maier, G. L., Fetter, R. D., Schneider-

Mizell, C. M., Truman, J. W., Zlatic, M., Cardona, A. and Sprecher, S. G. (2017). Organization of the Drosophila larval visual circuit. *Elife* **6**, e28387.

Luo, L., Gershow, M., Rosenzweig, M., Kang, K., Fang-Yen, C., Garrity, P. A. and Samuel, A. D. T. (2010). Navigational decision making in Drosophila thermotaxis. *Journal of Neuroscience* **30**, 4261–4272.

Sawin, E. P., Harris, L. R., Campos, A. R. and Sokolowski, M. B. (1994). Sensorimotor transformation from light reception to phototactic behavior in Drosophila larvae (Diptera: Drosophilidae). *J. Insect Behav.* **7**, 553.

Zars, T. (2017). Working Memory: It's a Gas, Gas, Gas. *Current Biology* **27**, R179–R181.

Figures

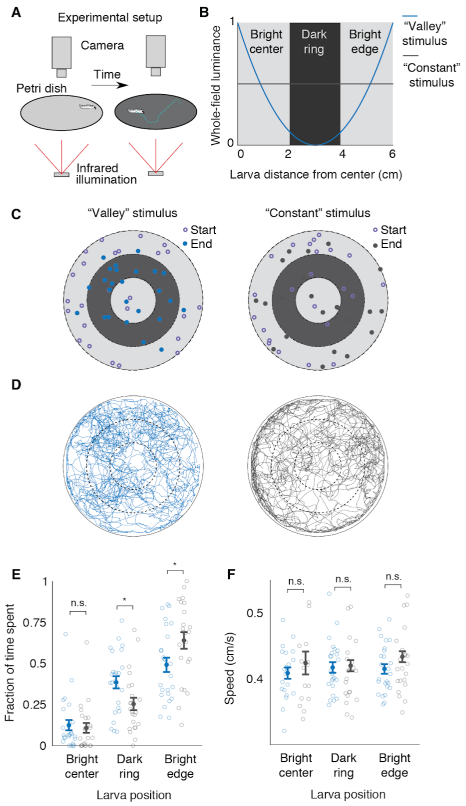

Figure 1 | *Drosophila* larvae can perform temporal phototaxis. (**A**) Experimental setup. The high-speed camera tracks the position of the freely crawling *Drosophila* larva (blue), using infrared illumination (red). A projector presents a spatially uniform, whole-field illumination to the animal from below. (**B**) For the "Valley" stimulus, the light intensity (λ; blue solid line) is given by $\lambda = (r-3)^2/9$, where r is the larva's radial distance to the center of the arena. For the "Constant" stimulus, λ (gray solid line) was set to 0.5 regardless of the larva's position. For all analyses, the arena is split in three concentric regions: the "Bright center" ($r = 0-2\ cm$), the "Dark ring" ($r = 2-4\ cm$), and the "Bright edge" ($r = 4-6\ cm$). (**C,D**) Starting and end positions as well as raw trajectories for the "Valley" (left panels) and the "Constant" stimulus (right panels); n = 25 larvae for the "Valley" stimulus and n = 23 larvae for the "Constant" stimulus. (**E,F**) Blue indicates "Valley" stimulus larvae; gray indicates "Constant" stimulus larvae. Open circles represent individual animals. (**E**) Average fraction of time larvae spent in each region. "Valley" stimulus larvae spent more time in the "Dark ring" region (p = 0.017, two-sided t-test) and less time in "Bright edge" region than "Constant" stimulus larvae (p = 0.031, two-sided t-test); n = 25 larvae for the "Valley" stimulus and n = 23 larvae for the "Constant" stimulus. (**F**) Average speed of larvae during the "Valley" stimulus and during the "Constant" stimulus (n.s. = not significant; p = 0.40, p = 0.86, p = 0.19 from left to right; two-sided t-tests). Note that not all larvae entered all regions during the experiment. For the "Valley" stimulus, out of n = 25 larvae, only 21 animals entered the "Bright" center and all 25 animals entered the other regions. For the control stimulus,

out of n = 23 larvae, 16 animals entered the “Bright” center region, 22 animals entered the “Dark” ring region, and 23 animals entered the “Bright” edge region. Error bars in (**E,F**) represent mean ± SEM.

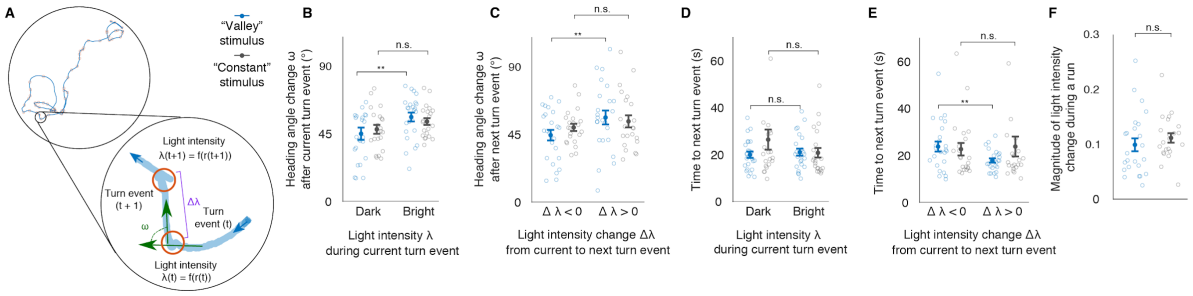

Figure 2 | Turning events modulate temporal phototaxis. (**A**) Sample larva trajectory (blue) and detected turn events (red circles). Inset shows two turn events at time *t* and time *t* + *1*. The intensity of the spatially uniform luminance (λ) is a function of the larva's distance from the center at that time. The green angle (ω) is the heading angle change during the turn event. The purple bracket is the change in light intensity between the two turn events. (**B–F**) Blue and gray indicate "Valley" and "Constant" stimulus larvae, respectively. Open circles represent data points for individual larvae. (**B**) Heading angle change after turn event as a function of current luminance λ. For "Dark" and "Bright": n = 24 and 24 larvae for the "Valley" stimulus and n = 21 and 22 larvae for the "Constant stimulus. (**C**) Heading angle change after next turn event grouped based on whether luminance will have increased or decreased since the current turn event. For Δλ < 0 and Δλ > 0: n = 24 and 24 larvae for the "Valley" stimulus and n = 23 and 23 larvae for the "Constant" stimulus. (**D**) Time to next turn event as a function of current luminance. For "Dark" and "Bright": n = 24 and 24 larvae for the "Valley" stimulus and n = 22 and 22 larvae for the "Constant stimulus. (**E**) Time to next turn event grouped based on whether luminance will have increased or decreased since the current turn event. For Δλ < 0 and Δλ > 0: n = 24 and 24 larvae for the "Valley" stimulus and n = 22 and 22 larvae for the "Constant" stimulus. "Dark" means that larvae were located within the "Dark" ring region. "Bright" indicates that larvae were located in the "Bright" center or the "Bright" edge regions. (**F**) Magnitude of change in light intensity between turn events i.e. during a run. Error bars indicate mean ± SEM.

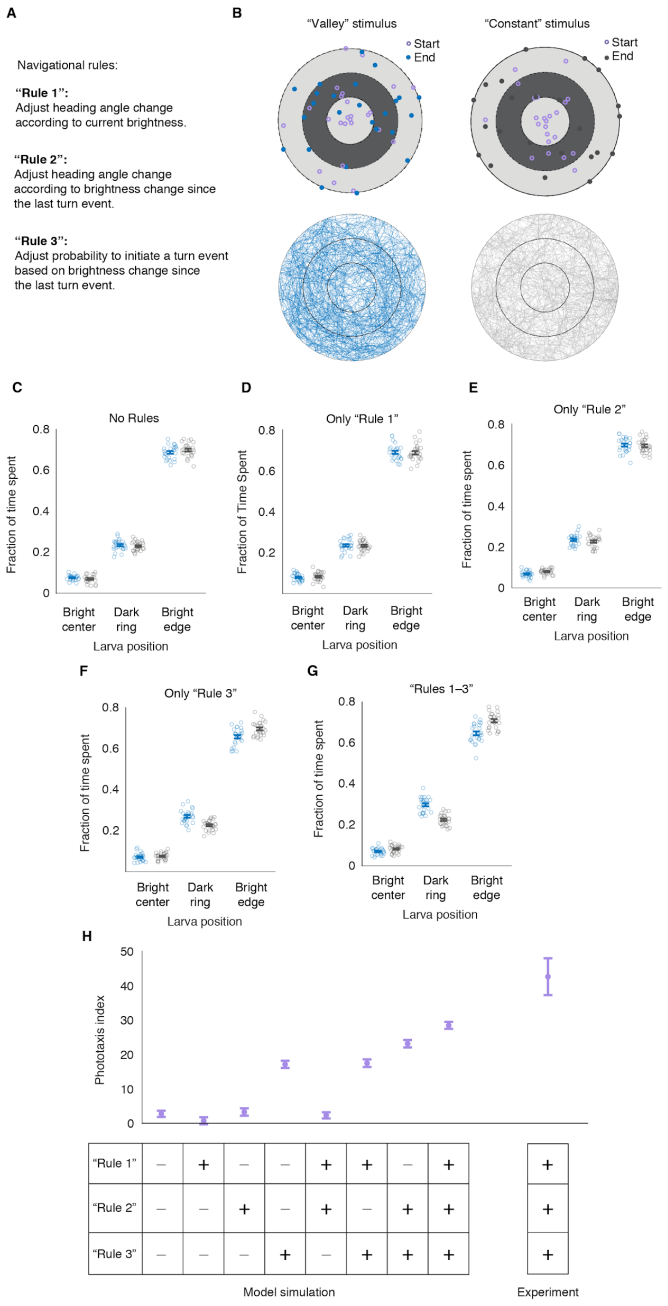

Figure 3 | Simulated larvae can replicate temporal phototaxis. (**A**) Description of three possible navigational rules larvae use during temporal phototaxis. (**B**) Simulated larvae employing all three rules for the "Valley" stimulus (left) and "Constant" stimulus (right). Start and end positions (top) and raw trajectories (bottom). (**C–G**). Average fraction of time simulated larvae spent in each region for different combinations of the three navigational rules. Blue and gray indicate "Valley" stimulus and "Constant" stimulus simulations; n = 25 simulated larvae. Error bars represent mean ± SEM. (**H**) Phototaxis index, comparing the eight simulated models with the experimental data. Error bars indicate mean ± 95% confidence interval.

Supplementary figures

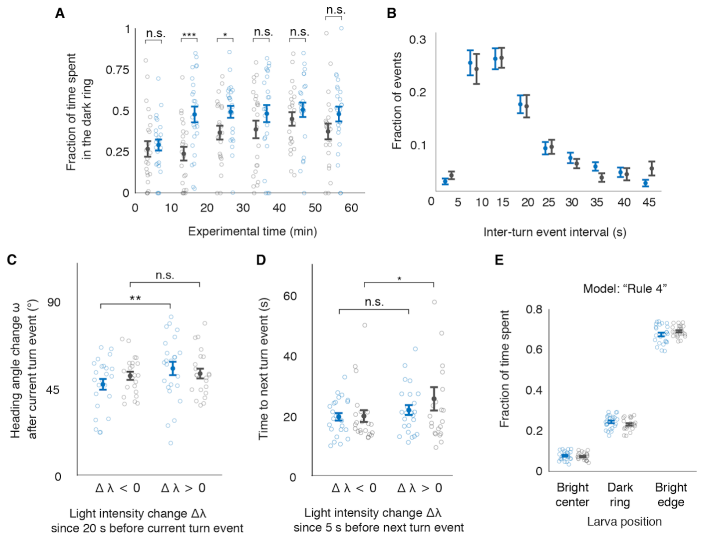

Supplementary Figure S1 | Additional analyses in relation to Fig. 1 and Fig. 2. (**A–D**). Blue indicates "Valley" stimulus larvae; gray indicates "Constant" stimulus larvae. Open circles represent individual animals. Error bars represent mean ± SEM. (**A**) Average fraction of time spent in the "Dark" ring, in 10-minute intervals of the experimental period; n = 25 for the "Valley" stimulus; n = 23 for the "Constant" stimulus. *p < 0.05, ***p < 0.001 (two-sided t-tests). (**B**) Distribution of inter-turn intervals. (**C**) Heading angle after next turn event depending on whether light intensity had increased or decreased since 20 s ago. (**D**). Time to next turn event depending on whether light intensity had increased or decreased since 5 s ago. *p < 0.05, **p < 0.01 (paired t-test). (**E**) Average fraction of time simulated larvae spent in each region when using "Rule 4", in which we adjust the probability of initiating a turn as a function of the current light intensity. Blue and gray dots and lines indicate simulated larvae navigating the "Valley" stimulus and the "Constant" stimulus, respectively; n = 25 simulated larvae. Error bars represent mean ± SEM over model runs.